Contributed Paper

# Numerical Analysis of Neoclassical Tearing Mode Stabilization by Electron Cyclotron Current Drive

HAYASHI Nobuhiko, ISAYAMA Akihiko, NAGASAKI Kazunobu[1)] and OZEKI Takahisa

*Naka Fusion Research Establishment,*
*Japan Atomic Energy Research Institute, Ibaraki 311-0193, Japan*
*[1)]Institute for Advanced Energy, Kyoto University, Kyoto 606-8501, Japan*

(Received 28 November 2003 / Accepted 22 April 2004)

Neoclassical tearing mode (NTM) stabilization by an electron cyclotron current drive (ECCD) has been studied by using the numerical model on the basis of the modified Rutherford equation coupled with the 1.5 D transport code and the EC code. The transport code solves the current diffusion equation, including the EC current profile. The background current modification and the resultant movement of rational surface by ECCD are taken into account. The EC code consists of the ray tracing method and the Fokker-Planck calculation. Undetermined parameters in the modified Rutherford equation are estimated from a comparison with the JT-60U experiments. Sensitivity of stabilization to the EC current location is investigated by simulation. The low EC current and peaked EC current profile mitigates the sensitivity, whereas the high EC current and peaked EC current profile moves the rational surface more largely via background current modification by the EC current and intensifies the sensitivity. The high EC current and broad EC current profile mitigates the sensitivity. The EC current necessary for the full stabilization is studied for ITER parameters. The necessary EC current strongly depends on the parameters of bootstrap current and ECCD terms in the modified Rutherford equation. Necessary ECCD power on ITER is evaluated on the basis of parameters estimated from comparisons with JT-60U experiments.

**Keywords:**
neoclassical tearing mode, stabilization, electron cyclotron current drive, simulation, experiment, tokamak

## 1. Introduction

Neoclassical tearing mode (NTM) softly limits the plasma beta or leads to disruption in long-pulse tokamak discharges. NTM stabilization is one of the crucial issues in tokamak reactors such as ITER [1]. NTM is driven by the lack of bootstrap current inside the magnetic island where the pressure profile is flattened. An additional current compensates for the lack of bootstrap current, and has a stabilizing effect on NTM. A localized current by an electron cyclotron wave (ECCD) is considered one of the effective methods to stabilize NTM. NTM stabilization by ECCD has been demonstrated experimentally in several tokamaks [2-5]. The stabilizing efficiency of ECCD is sensitive to the EC current profile and the relative location between the rational surface and the EC current. Optimum control of ECCD is necessary for effective stabilization. For the purpose of designing ECCD in ITER, the EC power required for NTM stabilization should be examined. An effective method to lower the required EC power moderates the demand for EC power. From these points of view, NTM stabilization by ECCD should be numerically studied in order to clarify the effective stabilization and the necessary ECCD power.

To investigate NTM stabilization by ECCD, the modified Rutherford equation [6] is generally used. The modified Rutherford equation is useful to analyze NTM behavior, such as the onset condition of NTM and the time evolution of NTM island width. In the modified Rutherford equation, however, there are several uncertainties relative to models, such as coefficients of models, model formulae, and so on. The NTM behavior may depend on the parameters of the applied model. In order to validate the models, a comparison of time evolution of NTM island width between the numerical results and the experimental ones has been done in several tokamaks. Ranges of the parameters in the modified Rutherford equation have been estimated by fitting the numerical results to the experimental ones, which are summarized in Ref. [6].

NTM stabilization by ECCD is sensitive to the relative location between the rational surface and the EC current. Precise adjustment of EC current location to the island center is required to achieve full stabilization. Moreover, the EC current may move the rational surface via background current

*author's e-mail: hayashin@fusion.naka.jaeri.go.jp*
*This article is based on the invited talk at the 20th JSPF Annual Meeting (Nov. 2003, Mito).*

modification by the EC current. This movement of the rational surface by ECCD makes the adjustment of EC current location to the island center further difficult. In order to take into account the background current modification by the EC current, the EC current is included in the calculation of the current diffusion equation. The modified Rutherford equation is coupled with the current diffusion equation. As a result, the effect of the movement of the rational surface by ECCD on the NTM stabilization can be examined.

An evaluation of the ECCD power necessary for the NTM stabilization on ITER has been done by Pustovitov [7]. Pustovitov showed that a modulated EC power of 28 MW is necessary to stabilize saturated islands of $m/n$ = 2/1 and 3/2 where $m$ and $n$ denote poloidal and toroidal mode numbers, respectively. Pustovitov also pointed out that early EC injection to growing islands can reduce the necessary EC power to 18 MW if the ion polarization current [8] has a large stabilizing effect on the NTM island. In a recent design of ITER [9,10], an initial installation of 20 MW EC power is planned for the NTM stabilization, and an additional power of 20 MW is considered as a possible upgrade option. Pustovitov's model was also based on the modified Rutherford equation. A specific set of parameters was used in the modified Rutherford equation. An ECCD power evaluation by use of experimentally-estimated parameters is necessary to improve the accuracy of the evaluation.

In this paper, three important results in the numerical analysis of NTM stabilization by ECCD are presented. The numerical model is based on the modified Rutherford equation coupled with the 1.5 dimensional (1.5 D) transport code. The transport code solves the current diffusion equation, including the EC current profile. The background current modification and the resultant movement of the rational surface by ECCD are taken into account. The EC current profile is modeled by a Gaussian distribution based on the results of the EC code [11]. First, in order to estimate undetermined parameters in the modified Rutherford equation, numerical results are compared with JT-60U experiments. Second, the sensitivity of the stabilization to the EC current location is studied by simulation. The effect of the movement of the rational surface by ECCD on the sensitivity is considered. Finally, the EC current necessary for NTM stabilization is investigated for the ITER parameters. Characteristics of the EC current necessary for the stabilization are shown. Based on the estimated parameters from the comparison with the JT-60U experiment, the ECCD power necessary in ITER is evaluated.

## 2. Numerical Model

NTM stabilization by ECCD is investigated by using a numerical model explained as follows. The time evolution of an island width of NTM is calculated by the modified Rutherford equation. The modified Rutherford equation is coupled with the 1.5 D transport code. In order to take into account the background current profile modification by the EC current, the current diffusion equation is calculated in the 1.5 D transport code. The EC current profile is modeled by a Gaussian distribution based on the results of the EC code [11]. In the next sub-section, details of the modified Rutherford equation are provided. Undetermined parameters in the modified Rutherford equation, which should be estimated from comparisons with experiments, are briefly summarized. The transport equations and the current diffusion equation used in the transport code are described in sub-section **2.2.** In the last sub-section, we explain the model for the EC current profile.

### 2.1 Modified Rutherford equation

The time evolution of a NTM island full-width, $W$, on the coordinate of the normalized minor radius, $\rho$, defined by the square root of the toroidal flux, $\Phi$, is calculated according to the modified Rutherford equation [6,12] as

$$\frac{\mathrm{d}W}{\mathrm{d}t} = \Gamma_{\Delta'} + \Gamma_{\mathrm{BS}} + \Gamma_{\mathrm{GGJ}} + \Gamma_{\mathrm{pol}} + \Gamma_{\mathrm{EC}}, \qquad (1)$$

$$\Gamma_{\Delta'} = k_{\mathrm{c}} \frac{\eta}{\mu_0} \Delta'(W) \left\langle |\nabla\rho|^2 \right\rangle, \qquad (2)$$

$$\Gamma_{\mathrm{BS}} = k_{\mathrm{BS}} \eta L_{\mathrm{q}} j_{\mathrm{BS}} \left\langle \frac{|\nabla\rho|}{B_{\mathrm{p}}} \right\rangle \frac{W}{W^2 + W_{\mathrm{d}}^2}, \qquad (3)$$

$$\Gamma_{\mathrm{GGJ}} = -k_{\mathrm{GGJ}} \frac{\eta}{\mu_0} \varepsilon_{\mathrm{s}}^2 \beta_{\mathrm{ps}} \frac{L_{\mathrm{q}}^2}{\rho_{\mathrm{s}} L_{\mathrm{p}}} \left(1 - \frac{1}{q_{\mathrm{s}}^2}\right) \left\langle |\nabla\rho|^2 \right\rangle \frac{1}{W}, \qquad (4)$$

$$\Gamma_{\mathrm{pol}} = -k_{\mathrm{pol}} \frac{\eta}{\mu_0} g(\varepsilon_{\mathrm{s}}, \nu_{\mathrm{i}}) \beta_{\mathrm{ps}} \left( \frac{\rho_{\mathrm{pi}} L_{\mathrm{q}}}{L_{\mathrm{p}}} \right)^2 \left\langle |\nabla\rho|^2 \right\rangle \frac{1}{W^3}, \qquad (5)$$

$$\Gamma_{\mathrm{EC}} = -k_{\mathrm{EC}} \eta \frac{L_{\mathrm{q}}}{\rho_{\mathrm{s}}} \left\langle \frac{|\nabla\rho|}{B_{\mathrm{p}}} \right\rangle \eta_{\mathrm{EC}} \frac{I_{\mathrm{EC}}}{a^2} \frac{1}{W^2}, \qquad (6)$$

where $\Gamma_{\Delta'}$, $\Gamma_{\mathrm{BS}}$, $\Gamma_{\mathrm{GGJ}}$, $\Gamma_{\mathrm{pol}}$, and $\Gamma_{\mathrm{EC}}$ represent the respective effects of the equilibrium current profile, the bootstrap current, the toroidal geometry (called Glasser-Green-Johnson effect [6]), the ion polarization current, and the EC current. The value of $k_{\mathrm{c}}$ is chosen as $k_{\mathrm{c}}$ = 1.2 based on the theory [6,8,12] and confirmed by low-beta experiments [13]. The coefficients, $k_{\mathrm{BS}}$, $k_{\mathrm{GGJ}}$, $k_{\mathrm{pol}}$, and $k_{\mathrm{EC}}$, are constant values of order unity. The neoclassical resistivity, $\eta$, and the bootstrap current density, $j_{\mathrm{BS}}$, are obtained according to Ref. [14]. The standard tearing stability index, $\Delta'(W)$, is calculated by the cylindrical model [15]. Here, $B_{\mathrm{p}}$, $\varepsilon_{\mathrm{s}}$, $\beta_{\mathrm{ps}}$, $\rho_{\mathrm{s}}$, $\rho_{\mathrm{pi}}$, and $a$ are the poloidal magnetic field, the inverse aspect ratio, the local poloidal beta, the rational surface position, the normalized poloidal larmor radius, and the plasma minor radius, respectively. The values of $\langle x\rangle$ are the flux surface averaged values of $x$ obtained on the plasma equilibrium without the island. The scale lengths, $L_{\mathrm{q}}$ and $L_{\mathrm{p}}$, are defined as $L_{\mathrm{q}} = (\mathrm{d}q/\mathrm{d}\rho)^{-1}$ and $L_{\mathrm{p}} = -(\mathrm{d}p/\mathrm{d}\rho)^{-1}$, respectively, where $q$ denotes the safety factor and $p$ the total plasma pressure. The width,

$W_d$, in Eq. (3) describes the characteristic island width resulting from the effect of the parallel and perpendicular heat transport, and is obtained by the transport threshold model [16] as

$$W_{\rm d} = 5.1\left(\frac{\chi_{\rm e\perp}}{\chi_{\rm e\parallel}}\right)^{1/4}\left(\frac{L_{\rm q}}{\varepsilon_{\rm s}\rho_{\rm s}n}\right)^{1/2}\rho_{\rm s}\,, \tag{7}$$

where $n$, $\chi_{\rm e\parallel}$, and $\chi_{\rm e\perp}$ are the toroidal mode number and the electron diffusivity parallel and perpendicular to the magnetic field, respectively. The value of $g(\varepsilon_{\rm s}, \nu_{\rm i})$ in Eq. (5) is a function of $\varepsilon_{\rm s}$ and the ion-ion collisional frequency, $\nu_{\rm i}$, and is assumed to be in the low collisional regime as $g(\varepsilon_{\rm s}, \nu_{\rm i}) = \varepsilon_{\rm s}^{3/2}$ [8]. In Eq. (1), for the sake of simplicity, the polarization term of Eq. (5) is taken to be stabilizing [8]. The localization efficiency of EC current, $\eta_{\rm EC}$, in Eq. (6) is given as [12]

$$\eta_{\rm EC} = \frac{\displaystyle\int {\rm d}\rho \oint \frac{{\rm d}\alpha}{2\pi}\cos(m\alpha)\langle\langle j_{\rm EC}\rangle\rangle}{\displaystyle\int {\rm d}\rho \oint \frac{{\rm d}\alpha}{2\pi}\langle\langle j_{\rm EC}\rangle\rangle}\,, \tag{8}$$

and is calculated numerically according to the EC current profile on the flux surface of an island structure, which is assumed to be reconstructed on the $\rho$ coordinate. The value of $\langle\langle j_{\rm EC}\rangle\rangle$ is the flux surface averaged value of $j_{\rm EC}$ on the island structure. The value of $I_{\rm EC}$ in Eq. (6) is the total amount of the EC current.

Undetermined parameters in Eq. (1), which should be estimated from comparisons with experiments, are briefly summarized as follows. The values of $k_{\rm BS}$, $k_{\rm GGJ}$, and $k_{\rm pol}$ vary depending on theoretical models [6,8,12,16], and those obtained experimentally in several tokamaks have various ranges of values [6]. The value of $k_{\rm EC}$, based on the theory, is about 6 [12], though this has not yet been experimentally confirmed. In high collisional plasmas, the usual classical formula [17] can be used for $\chi_{\rm e\parallel}$. However, in low collisional plasmas, the usual classical formula yields an unphysically large heat flux. A few models that limit the parallel heat transport (flux-limit model) have been proposed [4,16]. The value of $W_{\rm d}$ varies depending on these models. A typical model is considered in this paper. The parallel heat transport is limited by the effective parallel wavelength of the mode, $\lambda_\parallel \approx L_{\rm q}R_0/nW_{\rm d}$, as proposed by Fitzpatrick [16]; i.e., $\chi_{\rm e\parallel} \approx v_{\rm th,e}\lambda_\parallel$, where $v_{\rm th,e}$ is the electron thermal speed and $R_0$ is the major radius. The value of $W_{\rm d}$ calculated by the usual classical formula [17] for $\chi_{\rm e\parallel}$ gives the lower bound because the value of $W_{\rm d}$ is amplified by the flux-limit model. In the comparison with experiments, the value of $k_{\rm BS}$ can be estimated from the saturated island width because the saturation is almost determined by $\Gamma_{\Delta'}$ and $\Gamma_{\rm BS}$ in Eq. (1). Other parameters of $k_{\rm GGJ}$, $k_{\rm pol}$, and $W_{\rm d}$ can be estimated from the comparisons at small $W$, because the small island behavior strongly depends on the values of $k_{\rm GGJ}$, $k_{\rm pol}$, and $W_{\rm d}$, as shown in Eqs. (3-5). The value of $k_{\rm EC}$ can be estimated from the comparisons with experiments on the stabilization by ECCD.

### 2.2 1.5 D transport code

The modified Rutherford equation is coupled with the conventional transport code. The transport code consists of the 1 D transport and current diffusion equations on the MHD equilibrium of the Grad-Shafranov equation in the 2-D plane $(R, Z)$ without the island structure. The transport equations are the continuity equation for the deuterium ion density, and the power balance equations for electrons and ions, which are expressed as

$$\frac{\partial n_{\rm i}}{\partial t} = \frac{\partial}{V'\partial\rho}\left(V'\left\langle|\nabla\rho|^2\right\rangle D_{\rm i}\frac{\partial n_{\rm i}}{\partial\rho}\right) + S\,, \tag{9}$$

$$\frac{\partial}{\partial t}\left(\frac{3}{2}n_jT_j\right) = \frac{\partial}{V'\partial\rho}\left(V'\left\langle|\nabla\rho|^2\right\rangle n_j\chi_j\frac{\partial T_j}{\partial\rho}\right) + P_j\,, \tag{10}$$

where $j$ = i or e. The values of $D$, $\chi$, $S$, and $P$ denote the particle, heat diffusivities, and the particle and energy source densities, respectively. The value of $V$ is the plasma volume within the radius $\rho$ and $V' = {\rm d}V/{\rm d}\rho$. The diffusion equation of the parallel current density, $j$, is solved to take into account the background current modification and the variation of $\Delta'$ by the EC current, and is expressed as

$$\frac{\partial}{\partial t}\left(\rho\frac{\partial\Psi}{\partial\Phi}\right) = \frac{\partial}{\partial\rho}\left\{\frac{\eta}{\mu_0}D_{\rm c}\rho\frac{\partial}{\partial\rho}\left(E_{\rm c}\frac{\partial\Psi}{\partial\Phi}\right) - S_{\rm c}\right\}, \tag{11}$$

$$j = \frac{2\Phi_1}{\mu_0}D_{\rm c}\left\langle R^{-2}\right\rangle^{1/2}\rho\frac{\partial}{\partial\rho}\left(E_{\rm c}\frac{\partial\Psi}{\partial\Phi}\right) \tag{12}$$

where $D_{\rm c} = (\langle R^{-2}\rangle V')^{-2}$, $E_{\rm c} = \langle R^{-2}\rangle\langle B_{\rm p}^2\rangle(\partial V/\partial\Psi)^2$, and $S_{\rm c} = \eta\langle(j_{\rm BS} + j_{\rm EC}){\rm B}\rangle/2\Phi_1 RB_{\rm t}\langle R^{-2}\rangle$. The quantities $\Psi$ and $\Phi_1$ are the poloidal flux and $\Phi$ at $\rho = 1$, respectively.

### 2.3 EC current profile

The EC current profile is modeled by a Gaussian distribution based on the results of the EC code [11] for saving the calculation time. In the EC code, the EC ray trajectory is obtained by a standard ray tracing method, and the EC driven current profile is calculated by the relativistic Fokker-Planck equation. From EC code results, the EC current profile can be modeled by a Gaussian distribution as

$$j_{\rm EC} = j_{\rm EC0}\exp\left(-C_{\rm EC}\left(\frac{\rho-\rho_{\rm EC}}{W_{\rm EC}}\right)^2\right), \tag{13}$$

where $C_{\rm EC}$ = 4 ln 2, $j_{\rm EC0}$ is calculated from the total EC current $I_{\rm EC}$, $\rho_{\rm EC}$ is a peak location of the EC current profile, and $W_{\rm EC}$ is the full-width at half maximum of the EC current profile. In the results of EC code, the value of $W_{\rm EC}$ is determined not only by the beam divergence but also by the injection angles. Optimized injection angles create the peaked EC current profile [11]. The total EC current $I_{\rm EC}$ is almost proportional to the ECCD power.

## 3. Results

Three important results of the numerical analysis of

NTM stabilization by ECCD are shown. First, in order to estimate the undetermined parameters, numerical results are compared with JT-60U experiments. Second, the sensitivity of NTM stabilization by ECCD to the EC current location is studied by simulations. The effect of the movement of the rational surface via the background current modification by ECCD on sensitivity is considered. Finally, characteristics of the EC current necessary for NTM stabilization are investigated for ITER parameters. Parameter dependence of the necessary EC current is examined. The necessary ECCD power in ITER is evaluated based on the estimated parameters from the comparison with the JT-60U experiment.

### 3.1 Comparison with JT-60U experiments

Numerical results are compared with JT-60U experiments. The undetermined parameters $k_{\rm BS}$, $k_{\rm GGJ}$, $k_{\rm pol}$, $k_{\rm EC}$, and $W_{\rm d}$ in Eq. (1) are estimated by fitting to experimental results so that the root mean square error (RMSE) is minimized. Two discharges in JT-60 experiments are selected: one produces the NTM island growth (E36705), the other performs the stabilization by real-time control of ECCD (E41666 [2]). Parameters of these discharges are as follows: $R_0 \approx 3.3$ m, $a \approx 0.8$ m, $B_{\rm t} \approx 3.7$ T, and the plasma current $I_{\rm p}$ = 1.5 MA. A $m/n$ = 3/2 mode NTM is destabilized at $\beta_{\rm N} = \beta_{\rm t}$ [%] $aB_{\rm t}/I_{\rm p}$ [MA] $\approx 2$ for E36705 and 1.5 for E41666 by a neutral-beam (NB) injection of about 20 MW. Plasma parameters are $\bar{n}_{\rm e} \approx 2.4 \times 10^{19}$ m$^{-3}$, $\bar{T}_{\rm e} \approx 4.3$ keV, and $\bar{T}_{\rm i} \approx$ 6.9 keV for E36705, and $\bar{n}_{\rm e} \approx 2.4 \times 10^{19}$ m$^{-3}$, $\bar{T}_{\rm e} \approx 3.2$ keV, and $\bar{T}_{\rm i} \approx 5.4$ keV for E41666. The rational surface position of $q$ = 3/2 is $\rho_{\rm s} \approx 0.4$ in both experiments. A method to evaluate the island width in experiments is briefly explained as follows. The island width is assumed to be proportional to the square root of the radial magnetic perturbation, $\tilde{B}_{\rm r}$, on the basis of the cylindrical formula [18]; i.e., $W \propto C_{\rm W}\sqrt{\tilde{B}_{\rm r}}$ where $C_{\rm W}$ is a constant value. In the experiment, the value of $\tilde{B}_{\rm r}$ is estimated as $\tilde{B}_{\rm r} \approx |\dot{B}|/f$ where $\dot{B}$ is measured by saddle coils and $f$ is the mode frequency. The constant value $C_{\rm W}$ is chosen for fitting to the island width evaluated from the electron temperature perturbation profile measured by the electron-cyclotron-emission (ECE). On the other hand, conditions of numerical calculations are as follows. Plasma profiles of $n_{\rm e}$, $T_{\rm e}$, and $T_{\rm i}$ are assumed to be fixed to those experimentally measured at the start time of calculation. The time evolution of the plasma current profile and the MHD equilibrium are solved. An initial island width is given according to that in experiments.

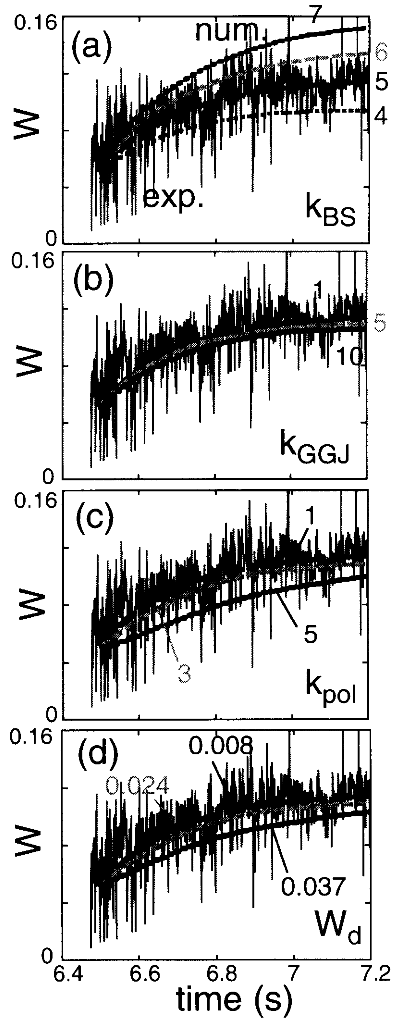


Fig. 1 Time evolution of island width $W$ evaluated from experiment and obtained from numerical calculations for a JT-60U discharge (E36705) where one of parameters (a) $k_{\rm BS}$, (b) $k_{\rm GGJ}$, (c) $k_{\rm pol}$ and (d) $W_{\rm d}$ is varied from a set of $k_{\rm BS}$ = 5, $k_{\rm GGJ} = k_{\rm pol}$ = 1 and $W_{\rm d}$ = 0.008, which almost fit numerical result to experiment.

The comparison at NTM island growth (E36705) is first investigated. Figure 1 shows the time evolution of island width $W$ evaluated from the experiment and obtained from numerical calculations where one of the parameters (a) $k_{\rm BS}$, (b) $k_{\rm GGJ}$, (c) $k_{\rm pol}$, or (d) $W_{\rm d}$ is varied from a set of $k_{\rm BS}$ = 5, $k_{\rm GGJ} = k_{\rm pol}$ = 1, and $W_{\rm d}$ = 0.008, which almost fit the numerical result to the experimental one (RMSE $\approx$ 0.02). As shown in Fig. 1(a), the numerical result strongly depends on $k_{\rm BS}$, and the value of $k_{\rm BS}$ is estimated as $k_{\rm BS} \approx 5$ to fit the numerical results to the experimental data. When the value of $k_{\rm GGJ}$ increases from 1 to 5 or 10, shown in Fig. 1(b), the island width decreases slightly. Thus, the value of $k_{\rm GGJ}$ is not important for the range of $k_{\rm GGJ} < 10$. When the value of $k_{\rm pol}$ increases from 1 to 3 or 5, shown in Fig. 1(c), the NTM growth becomes more gradual. The value of $k_{\rm pol}$ is estimated as $k_{\rm pol} < 3$ to fit to the experimental data. The value of $W_{\rm d}$ = 0.008 corresponds to that calculated by the usual classical formula [17] for $\chi_{\rm e\parallel}$. When the value of $W_{\rm d}$ increases from 0.008 to 0.024 or 0.037, shown in Fig. 1(d), the island grows more gradually. The value of $W_{\rm d}$ is estimated as $W_{\rm d} \leq 0.02$, which almost equals that calculated by Eq. (7) with the flux-limit model [16].

The comparison at the NTM stabilization by ECCD (E41666) is next investigated. With regard to the EC current profile, a Gaussian distribution of EC current density is applied on the basis of EC code results ($I_{\rm EC}$ = 52 kA, $W_{\rm EC}$ = 0.12). In the experiment, the real-time control of EC current location was applied to adjust the EC current location to the island center. However, there remains some degree of the misalignment between the EC current location and the rational surface due to an interval of ECE measured points of the electron temperature profile (2 cm) [2]. Here, we define the misalignment as $\Delta\rho = \rho_{EC} - \rho_s$. The maximum misalignment is $|\Delta\rho| = 0.02/a = 0.025$ for the experiment. In the numerical calculations, the EC current location traces the rational surface without ($\Delta\rho = 0$) and with a constant misalignment of $|\Delta\rho| = 0.025$. Figure 2 shows the time evolution of $W$ evaluated from the experiment and calculated numerically where $k_{EC}$ is varied for (a) $|\Delta\rho| = 0$ and (b) 0.025. Other parameters are fixed as

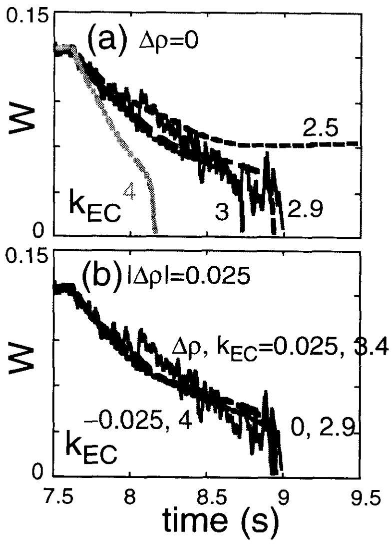


Fig. 2 Time evolution of island width $W$ evaluated from experiment and calculated numerically for a JT-60U discharge (E41666) where $k_{EC}$ is varied for misalignment of EC current location (a) $|\Delta\rho| = 0$ and (b) 0.025. Other parameters are fixed as $k_{BS} = 4.5$, $k_{GGJ} = k_{pol} = 1$ and $W_d = 0.02$.

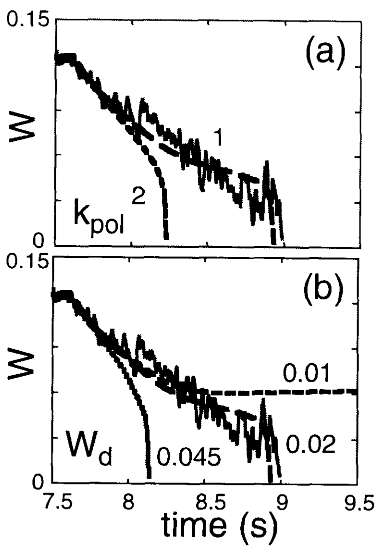


Fig. 3 Time evolution of island width $W$ evaluated from experiment and calculated numerically without misalignment of EC current location ($\Delta\rho = 0$) where one of parameters (a) $k_{pol}$ and (b) $W_d$ is varied from a set of $k_{BS} = 4.5$, $k_{GGJ} = k_{pol} = 1$, $k_{EC} = 2.9$ and $W_d = 0.02$, which almost fit numerical result to experiment.

$k_{BS} = 4.5$, $k_{GGJ} = k_{pol} = 1$, and $W_d = 0.02$. The value of $k_{BS}$ is estimated from the saturated island width at $t = 7.5$ s. This value of $k_{BS} = 4.5$ is smaller than that of 5.0 estimated in Fig. 1. The variation from $k_{BS} = 4.5$ to 5.0 does not much change the RMSE in Fig. 1(a). Thus, in these analyses, the value of $k_{BS}$ is estimated as $k_{BS} \approx 4$–5. In Fig. 2(a), the numerical results almost correspond to the experimental value for $k_{EC} \approx 3$ (RMSE $\approx 0.01$). On the other hand, in Fig. 2(b), the numerical results almost correspond to the experimental value for ($\Delta\rho$, $k_{EC}$) = (0.025, 3.4) and (–0.025, 4) (both RMSE $\approx 0.01$). From the results in Fig. 2, the value of $k_{EC}$ is estimated as $k_{EC} \approx 3$–4. Figure 3 shows the time evolution of $W$ evaluated from the experiment and calculated numerically without misalignment of the EC current location ($\Delta\rho = 0$) where one of the parameters (a) $k_{pol}$ and (b) $W_d$ is varied from a set of $k_{BS} = 4.5$, $k_{GGJ} = k_{pol} = 1$, $k_{EC} = 2.9$, and $W_d = 0.02$, which almost fit the numerical result to the experiment. In this case, similar to that in Fig. 1, the value of $k_{GGJ}$ does not much vary the numerical result, and is not important for the range of $k_{GGJ} < 10$. The value of $k_{pol}$ is increased from 1 to 2 as shown in Fig. 3(a). For larger values of $k_{pol}$ above 1, the island width decreases more slowly and deviates from the experimental value. The value of $k_{pol}$ is estimated as $k_{pol} \approx 1$. In Fig. 3(b), the value of $W_d$ is varied from 0.02 to 0.01 and 0.045. For both cases of $W_d$ (0.01 and 0.045), the variation of $W$ separates from the experimental value. The value of $W_d$ is estimated as $W_d \approx 0.02$, which almost corresponds to a value calculated from Eq. (7) with the flux-limit model.

The numerical model reproduces the JT-60U experimental results for a set of values of parameters in the modified Rutherford equation. Undetermined parameters are estimated from the comparison with the experiments. Estimated parameters are consistent between two discharges of the NTM island growth (E36705) and the stabilization by ECCD (E41666). From the comparisons between the numerical results and the JT-60U experiments, the estimated parameters are as follows: $k_{BS} \approx 4$–5, $k_{GGJ} < 10$ (not important), $k_{pol} \approx 1$, $k_{EC} \approx 3$–4, and $W_d \approx 0.02$ (almost corresponds to Eq. (7) with the flux-limit model).

These parameters are compared with ranges of parameters estimated in several tokamaks [6]. In Ref. [6], the parameter ranges were estimated as $a_{bs} \approx 0.4\ k_{BS}\varepsilon_s^{0.5}L_q/L_p \approx 0.5$–$0.9$, $a_{GGJ} \approx 0.8\ k_{GGJ}\varepsilon_s^2 L_q^2(1-q^{-2})/(\rho_s L_p) \approx 0.1$–$0.3$, $a_{pol} \approx 0.8\ \varepsilon_s^{1.5}(a\rho_{pi}L_q/L_p)^2 = 1$–$5\ \mathrm{cm}^2$, and $w_d \approx aW_d = 0.5$–$2$ cm. By using experimental conditions in two discharges of JT-60U (i.e., $\rho_s \approx 0.4$, $\varepsilon_s \approx 0.1$, $L_q \approx 0.6$, $L_p \approx 0.3$ and $\rho_{pi} \approx 5.6 \times 10^{-2}$), the parameters according to formulae in Ref. [6] are obtained for JT-60U experiments as $a_{bs} \approx 1$, $a_{GGJ} \approx 0.2$, $a_{pol} \approx 2\ \mathrm{cm}^2$, and $w_d \approx 2$ cm. These values are almost consistent with the parameter ranges estimated in Ref. [6].

## 3.2 Simulation study of the sensitivity of stabilization to the EC current location

The sensitivity of the NTM stabilization by ECCD to the EC current location is studied. The effect of the movement of the rational surface via the background modification by ECCD on the sensitivity is taken into account. In the numerical model, the current diffusion including the EC current of Eq. (11) is solved to evaluate the movement of the rational surface. Simulation of the 3/2 mode NTM stabilization by ECCD has been done for typical JT-60 superconducting tokamak parameters: $R_0 = 2.9$ m, $a = 0.85$ m, $B_t = 3.8$ T, and the plasma current $I_p = 3$ MA [19]. The parameters in Eq. (1) are set as $k_{BS} = 4$, $k_{GGJ} = 1$, $k_{pol} = 1$, $k_{EC} = 6$, and $W_d \approx 0.01$. Here, the value of $k_{EC} = 6$ is based on the theory [12], and is larger than the estimated value in JT-60U experiments. The value of $W_d \approx 0.01$ corresponds to that calculated by the classical formula [17] for $\chi_{e\|}$, and is smaller than that evaluated with the flux-limit model. These differences do not much change the characteristics of sensitivity of stabilization to the EC current location discussed here. The time evolution of plasma profiles is solved by Eqs. (9-10). Steady-state plasma parameters are $\beta_N \approx 1.8$, $\bar{n}_e \approx 4.2 \times 10^{19}$ m$^{-3}$, $\bar{T}_e \approx 6.4$ keV, and $\bar{T}_i \approx 7.5$ keV. The fundamental O-mode EC wave with a frequency of 110 GHz is launched from a position of $R = 3.7$ m and $Z = 0.95$ m.

Figure 4 shows the time evolution of island width $W$ (width between upper and lower lines) and rational surface $\rho_s$ (a middle line) for the following three cases of the EC current location: (a) inside $\rho_s$, (b) just on the island center, and (c) outside $\rho_s$ at $t = 10$ s, where the EC current width $W_{EC} = 0.045$ and the total EC current $I_{EC}/I_p \approx 0.02$ (peak ratio of the EC current density to the bootstrap current, $j_{EC}/j_{BS} \approx 1$). The EC current location is fixed in each case. The island width is decreased by an on-center EC current, and the NTM is fully stabilized as shown in Fig. 4(b). On the other hand, in Fig. 4(a) and (c), off-center EC currents can decrease island width, but not fully stabilize the NTM. As shown in Fig. 4, the rational surface $\rho_s$ moves away from the EC current location. The EC current moves the rational surface via background current profile modification. The EC current profiles become further off-center. This movement further decreases the stabilizing efficiency of the EC current. Figure 5 shows the time evolution of $W$ for the same three cases as those in Fig. 4 where $I_{EC}/I_p \approx 0.04$. Higher EC current induces larger movement of the rational surface. As a result, the island width at the high EC current in Fig. 5(c) (i.e., $W \approx 0.1$ at $t = 11$ s) is larger than that at the low EC current in Fig. 4(c) ($W \approx 0.05$) at the same time.

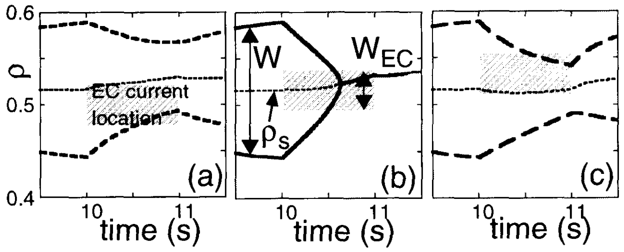


Fig. 4 Time evolution of island width $W$ (width between upper and lower lines) and rational surface $\rho_s$ (a middle line) for EC current location (a) inside $\rho_s$, (b) just on island center and (c) outside $\rho_s$ at $t = 10$ s, where EC current width $W_{EC} = 0.045$ and total EC current $I_{EC}/I_p \approx 0.02$ (peak ratio of EC current density to bootstrap current, $j_{EC}/j_{BS} \approx 1$).

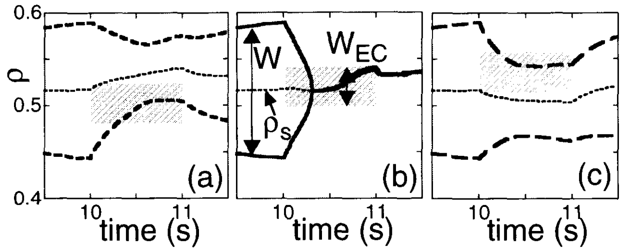


Fig. 5 Time evolution of island width $W$ for the same three cases as those in Fig. 4 where EC current is higher than in Fig. 4, $I_{EC}/I_p \approx 0.04$.

The conditions of full stabilization are investigated for various values of $I_{EC}$, $W_{EC}$, and the EC current location $\rho_{EC}$. Figure 6 shows stabilized regions on a plane of ($W_{EC}$, $\rho_{EC}$), in which the NTM can be fully stabilized, where (a) $I_{EC}/I_p \approx 0.02$, (b) 0.03, and (c) 0.04. At the low EC current of $I_{EC}/I_p \approx 0.02$ in Fig. 6(a), the NTM is not fully stabilized for a large value of EC current width such as $W_{EC} > 0.053$. The stabilized region appears and the range of $\rho_{EC}$ in the stabilized region becomes wide for small $W_{EC} < 0.053$ because the localization efficiency of EC current, $\eta_{EC}$ of Eq. (8), becomes large for small $W_{EC}$. From a different viewpoint, the EC current density has a threshold value required for full stabilization. At $W_{EC} = 0.053$, the ratio of a peak value of the EC current density to the bootstrap current density at the rational surface, $j_{EC}/j_{BS}$, is about 0.7. For the stabilized region wide for the $\rho_{EC}$ direction, the sensitivity of the stabilization on the EC current location is weak. Low power and peaked current profile mitigates the sensitivity. On the other hand, at a high EC current of $I_{EC}/I_p \approx 0.04$ shown in Fig. 6(c), the high EC current density moves the rational surface more largely and narrows the range of $\rho_{EC}$ in the stabilized region for small $W_{EC}$. The high current and the peaked current profile intensify the sensitivity as a result of the background current modification by the EC current. For the larger $W_{EC}$ in Fig. 6(c), the range of $\rho_{EC}$ in the stabilized region becomes wider. The high EC current and broad EC current profile mitigates the sensitivity. This effect of the movement of the rational surface via the background modification by the EC current on the sensitivity will be studied experimentally in the future. From these results, the real-time control of EC current location is required for

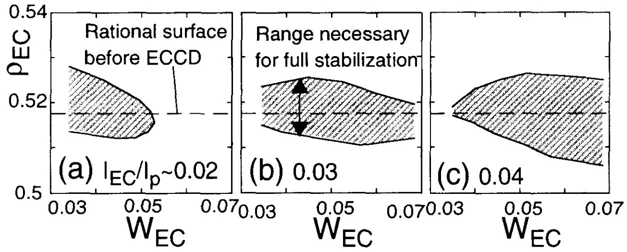


Fig. 6 Stabilized regions on a plane of ($W_{EC}$, $\rho_{EC}$), in which the NTM can be fully stabilized, where (a) $I_{EC}/I_p \approx 0.02$, (b) 0.03 and (c) 0.04.

effective stabilization. Careful adjustment of ECCD, such as current amount and width, is necessary for real-time control.

### 3.3 EC current necessary for stabilization in ITER

Characteristics of the EC current necessary for NTM stabilization are shown. Numerical analyses have been performed for almost the same parameters as those in the scenario of ITER inductive operation [20]; i.e., $R_0$ = 6.2 m, $a$ = 2 m, $B_t$ = 5.3 T, $I_p$ = 15 MA [21]. Plasma profiles of $n_e$, $T_e$, and $T_i$ are fixed. Plasma parameters are $\beta_N \approx 1.8$, $\bar{n}_e \approx 1.0 \times 10^{20}$ m$^{-3}$, $\bar{T}_e \approx 9.1$ keV, and $\bar{T}_i \approx 8.3$ keV. The rational surface positions are $\rho_s \approx 0.76$ for $q$ = 3/2 and 0.9 for 2/1. The fundamental O-mode wave with a frequency of 170 GHz is launched from a position of $R$ = 6.5 m and $Z$ = 4.0 m, which almost corresponds to an upper launcher in the design of ITER [9]. The full-width at half maximum of EC current profiles, $W_{EC}$, is about 0.04. The EC current profile is assumed to locate just at the island center and to trace the movement of the rational surface.

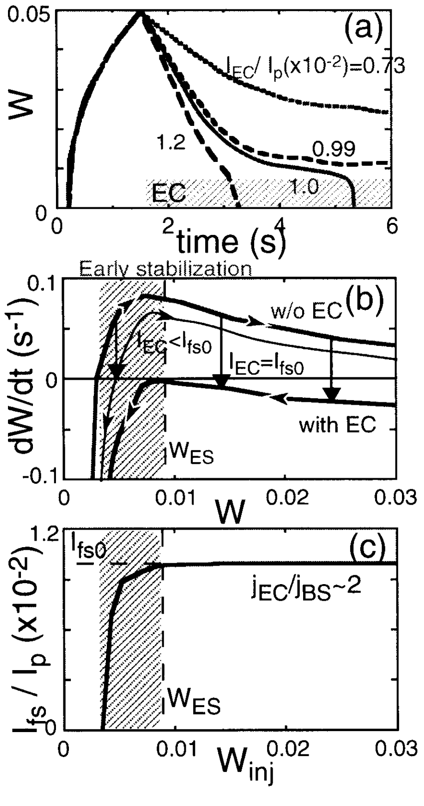


Fig. 7 (a): Time evolution of island width $W$ for various values of EC current $I_{EC}/I_p$. EC current above $I_{EC}/I_p \approx 0.01$ can fully stabilize NTM. (b): Growth rate d$W$/d$t$ as a function of island width $W$ with (lower broad and thin lines) and without (upper broad line) ECCD where $I_{fs0}/I_p \approx 0.01$. Lower broad line represents a case where island of $W > W_{ES}$ can be fully stabilized by EC current of $I_{EC} = I_{fs0}$. Thin line represents a case where island of $W < W_{ES}$ can be fully stabilized by $I_{EC} < I_{fs0}$. Early EC injection to growing island of $W < W_{ES}$ can reduces necessary EC current for full stabilization of NTM island. (c): Necessary EC current for full stabilization, $I_{fs}$, as a function of island width at EC injection, $W_{inj}$. Values of $I_{fs0}$ and $W_{ES}$ are important for NTM stabilization by ECCD.

Figure 7(a) shows the time evolution of 3/2 mode NTM island width $W$ for various values of the EC current $I_{EC}/I_p$. The EC current above $I_{EC}/I_p \approx 0.01$ can fully stabilize the NTM as shown in Fig. 7(a). Here, the condition for the full stabilization is defined as $I_{EC} \geq I_{fs}$. Figure 7(b) shows the growth rate d$W$/d$t$ against the island width $W$ with and without ECCD where $I_{fs0}/I_p \approx 0.01$. At the condition of $I_{EC} = I_{fs0}$ in Fig. 7(b) (lower broad line), there is a peak at $W = W_{ES} \approx 0.01$. If the island width is once larger than $W_{ES}$, the EC current of $I_{fs0}$ is required to decrease the island width below $W_{ES}$. The value of $I_{fs0}$ is the threshold value of stabilization for the case of $W > W_{ES}$; i.e., $I_{fs} = I_{fs0}$ for $W > W_{ES}$. On the other hand, if the island width is smaller than $W_{ES}$, EC current less than $I_{fs0}$ is required to fully stabilize the NTM, as shown at the condition of $I_{EC} < I_{fs0}$ in Fig. 7(b) (thin line). Early EC injection to the growing island of $W < W_{ES}$ can reduce the necessary EC current for the full stabilization; i.e., $I_{fs} < I_{fs0}$ for $W < W_{ES}$. The possibility of lowering the required EC power by early injection to the growing island was first pointed out by Pustovitov [7]. Figure 7(c) shows the EC current necessary for full stabilization, $I_{fs}$, as a function of island width at the EC injection, $W_{inj}$. The values of $I_{fs0}$ and $W_{ES}$ are important for the NTM stabilization by ECCD.

In order to estimate the necessary EC current, it is important to clarify the dependence of $I_{fs0}$ and $W_{ES}$ on the undetermined parameters $k_{BS}$, $k_{GGJ}$, $k_{pol}$, $k_{EC}$, and $W_d$ in Eq. (1). Figure 8 shows the dependence of $I_{fs0}/I_{fs00}$ on (a) $k_{BS}$ and (b) $W_d$ when one of the parameters is varied from the base set of parameters $k_{BS}$ = 4, $k_{GGJ} = k_{pol}$ = 1, $k_{EC}$ = 4, and

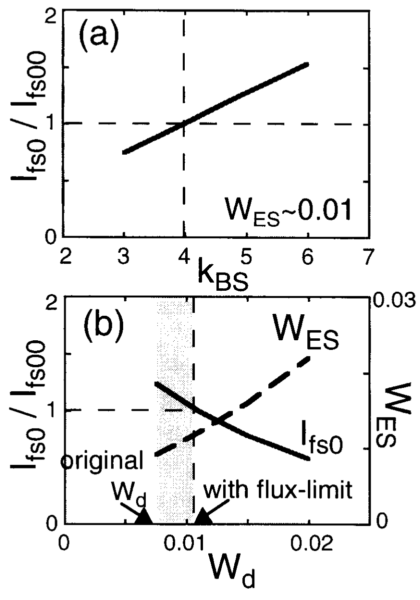


Fig. 8 Dependence of $I_{fs0}$ and $W_{ES}$ on (a) $k_{BS}$ and (b) $W_d$ where one of the parameters $k_{BS}$ and $W_d$ is varied from a set of parameters of $k_{BS}$ = 4, $k_{GGJ} = k_{pol}$ = 1, $k_{EC}$ = 4, $W_d \approx 0.01$, at which $I_{fs0} = I_{fs00}$. In Fig. (a), $W_{ES}$ is not much varied from about 0.01. In Fig. (b), value of $W_d$ at left side of shaded region is calculated from Eq. (7) without flux-limit model, while $W_d$ at right side is with flux-limit model.

$W_d \approx 0.01$ in each figure, and $I_{fs00}$ is a value of $I_{fs0}$ for the base set of parameters. In Fig. 8(b), the value of $W_d$ at the left side of the shaded region is calculated from Eq. (7) without the flux-limit model, while $W_d \approx 0.01$ at the right side is with the flux-limit model. The value of $I_{fs0}$ is slightly reduced by increasing the stabilizing coefficients of $k_{GGJ}$ and $k_{pol}$. Thus, the dependence on $k_{GGJ}$ and $k_{pol}$ is weak and is not shown here. In Fig. 8(a), the value of $W_{ES}$, about 0.01, does not much vary. As shown in Fig. 8(a), the value of $I_{fs0}$ is varied by 20% for a range of $k_{BS} \approx$ 4–5. The value of $I_{fs0}$ strongly depends on the destabilizing bootstrap coefficient of $k_{BS}$. In Fig. 8(b), the value of $I_{fs0}$ decreases and that of $W_{ES}$ increases with increasing the value of $W_d$. This is because the destabilizing bootstrap term in Eq. (1) has a maximum value proportional to $W_d^{-1}$ at the island width of $W = W_d$ as shown in Eq. (3). As is easily seen in Eq. (6), the value of $I_{fs0}$ is inversely proportional to $k_{EC}$. The necessary EC current strongly depends on the parameters of bootstrap current and ECCD terms in the modified Rutherford equation. The exact values of $k_{BS}$, $k_{EC}$, and $W_d$ are required to estimate the necessary EC current.

Based on the parameters estimated from the comparison with the JT-60U experiment, the necessary ECCD power in ITER is evaluated. Parameters used in the ITER analysis are as follows: $k_{BS} \approx 4$, $k_{GGJ} \approx 1$, $k_{pol} \approx 1$, $k_{EC} \approx 4$, and $W_d \approx 0.01$. The values of the important parameters $k_{BS}$ and $W_d$ are almost the same as those suggested in Ref. [6]; i.e., $a_{bs} \approx 0.4\, k_{BS}\varepsilon_s^{0.5}L_q/L_p \approx 1$ and $w_d \approx 2$ cm for ITER profiles [21]. For the set of parameters, values of $I_{fs0} \approx 74$ kA for the 3/2 mode and 54 kA for the 2/1 mode are obtained. The value of $I_{fs0}$ for the 3/2 mode is higher than that for the 2/1 mode in the present conditions; i.e., a peak value of the destabilizing bootstrap term $\Gamma_{BS}$ of Eq. (3) is almost proportional to $L_q j_{BS}/W_d$, and the value of $L_q j_{BS}/W_d$ for the 3/2 mode is 1.3 times larger than that for the 2/1 mode [21]. From the EC code results, the EC power is proportional to the EC current as $P_{EC}$ [MW] $\approx 0.23\, I_{EC}$ [kA] for the 3/2 mode and $P_{EC}$ [MW] $\approx 0.24\, I_{EC}$ [kA] for the 2/1 mode . An ECCD power of 30 MW (17 MW for the 3/2 mode and 13 MW for the 2/1 mode) is required for the full stabilization of both the 3/2 and 2/1 modes on ITER. Our estimation of the necessary ECCD power is slightly larger than that by Pustovitov [7], in which the EC power of 28 MW is shown to be sufficient in the case without early injection to the growing island. Parameters in the modified Rutherford equation used in Pustovitov's study were as follows: $k_{BS} \approx 4$, $k_{GGJ} \approx 7$, $k_{pol} \approx 9$, $k_{EC} \approx 3$, and $W_d \approx 0.02$. The value of $W_d$ is about twice larger than that used in our study, while $k_{EC}$ is smaller than our value. The value of $g(\varepsilon_s, \nu_i)$ in Eq. (5) for the 2/1 mode was assumed to be in the high collisional regime, given that $g(\varepsilon_s, \nu_i) = 1$ in Pustovitov's study. These differences cause slight variance between Pustovitov's study and ours. In our results on the EC code, the value of $W_{EC}$ is about 0.04. However, a value of $W_{EC} \approx 0.02$ can be obtained if both the toroidal and poloidal injection angles of ECCD are optimized as indicated in Ref. [11]. Because the localized efficiency of the EC current, $\eta_{EC}$ of Eq. (8), is 2.5 times larger for $W_{EC} = 0.02$ than for $W_{EC} = 0.04$ [21], the necessary ECCD power can be reduced to 12 MW for $W_{EC} = 0.02$. Optimizing injection angles is important for the reduction of necessary ECCD power. Additionally, when the ECCD is injected to the growing island below $W_{ES}$, the required EC power can be lower than 12 MW. However, the estimated value of $W_{ES}$ is about 0.01 ($\approx$ 2 cm), as mentioned above. An island width below 2 cm seems to be small for early injection under the present experimental condition. Pustovitov showed that early EC injection to the growing islands can reduce the necessary EC power from 28 MW to 18 MW [7]. This reduction was, however, mainly caused by the large stabilizing effect of the ion polarization current term of Eq. (5) with $g(\varepsilon_s, \nu_i) = 1$ in the high collisional regime. A transition regime of function $g(\varepsilon_s, \nu_i)$ from $g(\varepsilon_s, \nu_i) = \varepsilon_s^{3/2}$ to 1 has not been clarified yet [7]. Thus, we adopted the small stabilizing effect of the ion polarization current with $g(\varepsilon_s, \nu_i) = \varepsilon_s^{3/2}$ for evaluation of the necessary ECCD power.

## 4. Summary

NTM stabilization by ECCD has been studied by using the numerical model on the basis of the modified Rutherford equation coupled with the 1.5 D transport code and the EC code. The transport code solves the current diffusion equation including the EC current profile. The background current modification and the resultant movement of the rational surface by ECCD are taken into account. The EC code consists of the ray tracing method and the Fokker-Planck calculation. The EC current profile is modeled by a Gaussian distribution based on results of the EC code for saving calculation time. Three important results have been obtained, as follows. Numerical results are compared with JT-60U experimental ones. The numerical model reproduces the JT-60U experimental results for a set of values of parameters in the modified Rutherford equation. Undetermined parameters in the modified Rutherford equation are estimated from the comparison with the JT-60U experiments. Sensitivity of the stabilization to the EC current location is investigated by simulation. The low EC current and peaked EC current profile mitigates the sensitivity, whereas the high EC current and peaked EC current profile moves the rational surface more largely via background current modification by the EC current and intensifies the sensitivity. The high EC current and broad EC current profile mitigates the sensitivity. As a result, real-time control of EC current location is required for effective stabilization. In the real-time control of ECCD, careful adjustment of the EC current amount and width is necessary. The EC current necessary for full stabilization is studied for ITER parameters. Parameter dependence of the necessary EC current is shown. The necessary EC current strongly depends on the parameters of bootstrap current and ECCD terms in the modified Rutherford equation. Necessary ECCD power on ITER is evaluated as 30 MW on the basis of parameters estimated from comparisons with JT-60U experiments. The necessary ECCD power can be reduced to 12 MW when the

EC current width is decreased by optimizing both toroidal and poloidal injection angles of ECCD. In the present analysis, the error of the estimated ECCD power is about 20% (from Fig. 8(a)) because the estimated value of $k_{BS}$ has a range of $k_{BS} \approx 4$–5. Precise estimation of the parameters for more JT-60U experiments is our future work.

## Acknowledgments

We would like to thank Drs. T. Takizuka, K. Hamamatsu, T. Suzuki, and T. Oikawa for fruitful discussion and support.

## References

[1] ITER Physics Basis Editors *et al.*, Nucl. Fusion **39**, 2137 (1999).
[2] A. Isayama *et al.*, Nucl. Fusion **43**, 1272 (2003).
[3] K. Nagasaki *et al.*, Nucl. Fusion **43**, L7 (2003).
[4] H. Zohm *et al.*, Nucl. Fusion **41**, 197 (2001).
[5] R. Prater *et al.*, Nucl. Fusion **43**, 1128 (2003).
[6] O. Sauter *et al.*, Phys. Plasmas **4**, 1654 (1997).
[7] V.D. Pustovitov *et al.*, *Proc. 18th Int. Conf. on Plasma Phys. Control. Fusion Research* (Sorrento, 2000), IAEA-CN-77/ITERP/07.
[8] H.R. Wilson *et al.*, Plasma Phys. Control. Fusion **38**, A149 (1996).
[9] R. Aymar, Fusion Eng. Des. **55**, 107 (2001).
[10] T. Imai, Fusion Eng. Des. **55**, 281 (2001).
[11] K. Hamamatsu and A. Fukuyama, Plasma Phys. Control. Fusion **42**, 1309 (2000).
[12] C.C. Hegna and J.D. Callen, Phys. Plasmas **4**, 2940 (1997).
[13] R.B. White *et al.*, Phys. Fluids **20**, 800 (1977).
[14] S.P. Hirshman and D.J. Sigmar, Nucl. Fusion **21**, 1079 (1981).
[15] J. Wesson, *Tokamaks* (Oxford Engineering Science Series 48), Oxford University Press, Oxford, 335 (1997).
[16] R. Fitzpatrick, Phys. Plasmas **2**, 825 (1995).
[17] S.I. Braginskii, "Transport Process in a Plasma" in Reviews of Plasma Physics, Consultants Bureau, New York, **1**, 205 (1965).
[18] A. Isayama *et al.*, Plasma Phys. Control. Fusion **41**, 35 (1999).
[19] N. Hayashi *et al.*, J. Plasma Fusion Res. SERIES **5**, 519 (2002).
[20] A. Polevoi *et al.*, J. Plasma Fusion Res. SERIES **5**, 82 (2002).
[21] N. Hayashi *et al.*, Nucl. Fusion **44**, 477 (2004).